Modeling the Optical Constants of $Al_xGa_{1-x}As$ alloys

A. D. Rakić, A. B. Djurišić*, E. Herbert Li* and M. L. Majewski

Department of Computer Science and Electrical Engineering,
The University of Queensland, Brisbane QLD 4072, Australia
*Department of EEE, University of Hong Kong,
Pokfulam Road, Hong Kong

Abstract— **Extension of Adachi's model with a Gaussian-like broadening function instead of a Lorentzian one is used to model the optical dielectric function of the alloy $Al_xGa_{1-x}As$. Gaussian-like broadening is accomplished by replacing the damping constant in the Lorentzian line shape with a frequency dependent expression. In such a manner, the comparative simplicity of analytic formulae of the model is preserved, while the accuracy becomes comparable to more intricate models, and/or models with a significantly greater number of parameters. The employed model describes accurately the optical dielectric function in the spectral range from 1.5 to 6.0 eV in the entire alloy composition range. Relative rms error obtained for the refractive index is below 2.2% for all compositions.**

I. Introduction

The alloy system $Al_xGa_{1-x}As/GaAs$ is of great technological importance in fabrication of various optoelectronic devices. Optical properties of solids are often described in terms of the complex optical dielectric function $\epsilon(\omega) = \epsilon_1(\omega) + \epsilon_2(\omega)$. Problem with experimental data is that they are not expressed as continuous analytic functions of the electronic energy gaps and the alloy composition x. Therefore, it is required to model the experimental data with an analytical model [1-3] The employed model must be simple and concise, and at the same time give reasonably good approximation of the optical spectra of investigated materials.

Adachi's model [4], [5] is relatively simple model which describes optical dielectric function with terms attributed to four energy gaps ($E_0, E_0+\Delta_0, E_1, E_1+\Delta_1$) and damped harmonic oscillators describing contributions from higher lying transitions ($E_0', E_2(X), E_2(\Sigma)$). However, Adachi's model is not very accurate, and several modifications have been proposed recently [1], [6-10]. Jenkins [6] obtained better agreement with experimental data by introducing exponential decay of matrix elements which are taken to be constant over the Brillouin zone in Adachi's model. However, this model gives good agreement with experimental data only in the narrow range, and for AlAs calculated values differ from experimental ones for a constant amount below 3 eV. Zheng *et al.* [10] have recently proposed modification of Adachi's model which includes excitonic terms at E_1 and $E_1 + \Delta_1$, gives new expression for the contribution of the indirect gap and introduces the Lorentzian lifetime broadening in a different manner. However, since model parameters (except the fundamental bandgap) are assumed to be linear functions of composition, this model does not yield the good agreement with experimental data for higher aluminum content ($x \geq 0.7$).

Kim *et al.* [11-13] have proposed an accurate but rather complicated model, which can include either Lorentzian or Gaussian broadening. Different types of broadening are accomplished by varying certain parameter in the expression for frequency dependent damping constant. The experimental data for $Al_xGa_{1-x}As$ in energy range from 1.5 eV to 6.0 eV and compositions from $x = 0.0$ to $x = 0.8$ in steps 0.1 and $x = 1$ were fitted with 119 parameters. Obtained relative rms error for the refractive index using this model is below 2.5% for all compositions [12].

Model of Kim *et al.* is much more complex than the Adachi's model (and contains a large number of adjustable parameters), still the improvement in accuracy is obtained mainly through replacing the Lorentzian broadening function with Gaussian one. With simple Lorentzian broadening function this model doesn't provide the good agreement with experimental data in the vicinity of the direct edge and below. The fact that Lorentzian broadening doesn't accurately describe the optical spectrum has already been recognized and discussed[1], [11], [14], [15]. Rakić and Majewski [1] have shown that Adachi's model with Gaussian-like broadening function describes accurately dispersion and absorption in GaAs and AlAs even in the vicinity of the E_0 where the original model of Adachi is highly inaccurate.

In this paper we show that a comparatively simple model of Rakić and Majewski [1] can be succesfully applied to model the optical spectrum of ternary alloys, in particular $Al_xGa_{1-x}As$, with accuracy similar to that of significantly more intricate model of Kim *et al.* Also, we compare two ways of determinig the parameters of the model for ternary compaunds. First approach is to determine the model parameters for particular compositions, and then to find the optimal function describing the dependence of the model parameters on the alloy composition x. The second approach is to simultaneously fit the data sets for all available compositions in order to minimize the discrepancies between calculated and experimental data over the entire energy and composition range. Our results clearly show that simultaneous fitting was needed to provide accurate values of optical functions. Finally, we discuss what was the

0-7803-4513-4/99/$10.00 © 1999 IEEE

advantage of using the global optimizing routine (namely our acceptance-probability-controlled simulated annealing algorithm [2], [3]) compared to clasical fitting algorithms, and how it effected the reliability of the final model parameters.

II. Model of the dielectric function

We shall briefly discribe the applied model for the dielectric function. The dielectric function in Adachi's model is represented by the sum of terms describing transitions at critical points (CPs) in joint density of states. In the modification proposed by Rakić and Majewski [1] damping constants Γ_i are replaced with frequency dependent expression $\Gamma_i'(\omega)$.

A. E_0 and $E_0+\Delta_0$ transitions

Under the parabolic band assumption, contributions of three-dimensional M_0 CPs E_0 and $E_0+\Delta_0$ are given by

$$\epsilon^{\mathrm{I}}(\omega) = AE_0^{-3/2}\left[f(\chi_0)+\frac{1}{2}\left(\frac{E_0}{E_0+\Delta_0}\right)^{3/2} f(\chi_{0s})\right], \quad (1)$$

where

$$f(y) = y^{-2}[2-(1+y)^{1/2}-(1-y)^{1/2}], \quad (2)$$

$$\chi_0 = \frac{\hbar\omega+i\Gamma_0}{E_0}, \quad (3)$$

$$\chi_{0s} = \frac{\hbar\omega+i\Gamma_0}{E_0+\Delta_0}, \quad (4)$$

where A and Γ_0 are strength and damping constant of the E_0 and $E_0+\Delta_0$ transitions, respectively.

B. E_1 and $E_1+\Delta_1$ transitions

For contributions of the two-dimensional M_0 CPs E_1 and $E_1+\Delta_1$, by taking the matrix element to be constant with respect to energy, Adachi obtained following expression

$$\epsilon^{\mathrm{II}}(\omega) = -B_1\chi_1^{-2}\ln(1-\chi_1^2) - B_{1s}\chi_{1s}^{-2}\ln(1-\chi_{1s}^2) \quad (5)$$

where

$$\chi_1 = \frac{\hbar\omega+i\Gamma_1}{E_1}, \quad (6)$$

$$\chi_{1s} = \frac{\hbar\omega+i\Gamma_1}{E_1+\Delta_1}, \quad (7)$$

$B_1(B_{1s})$ and Γ_1 are strength and damping constant of the E_1 and $E_1+\Delta_1$ transitions, respectively. Contribution of the Wannier type 2D excitons (discrete series of exciton lines at the E_1 and $E_1+\Delta_1$ CPs) is given by

$$\epsilon^{\mathrm{III}}(\omega) = \sum_{n=1}^{+\infty}\frac{1}{(2n-1)^3}\left(\frac{B_{1x}}{E_1-[G_1/(2n-1)^2]-\hbar\omega-i\Gamma_1} + \frac{B_{2x}}{(E_1+\Delta_1)-[G_{1s}/(2n-1)^2]-\hbar\omega-i\Gamma_1}\right), \quad (8)$$

where B_{1x} and B_{2x} are the strengths and G_1 and G_{1s} are Rydberg energies of E_1 and $E_1+\Delta_1$ exciton, respectively. Here it was assumed that $G_1 = G_{1s} = 0$ [1]. Summation of the excitonic terms is performed until the contribution of the next term is less than 10^{-4}.

TABLE I

Parameters describing composition dependence of four lowest critical points $E_0, E_0+\Delta_0, E_1$ and $E_1+\Delta_1$ according to Kim *et al.* [*Phys. Rev. B* **47**, 1876 (1993)].

parameter	$E(0)$	$E(1)-E(0)$	c_0	c_1
E_0	1.410	1.583	0.2242	-1.4235
$E_0+\Delta_0$	1.746	1.455	0.1931	-1.2160
E_1	2.926	0.962	-0.2124	-0.7850
$E_1+\Delta_1$	3.170	0.917	-0.0734	-0.9393

C. E_0', $E_2(X)$ and $E_2(\Sigma)$ transitions

The origin of transitions E_0', $E_2(X)$ and $E_2(\Sigma)$ is not completely clear, since they do not correspond to a single, well defined CP. However, these features can be adequately modeled with damped harmonic oscillators, characterized with energy E_j, oscillator strength $f_j = \sqrt{C_j E_j^2}$ and damping constant Γ_j, $j = 2,3,4$

$$\epsilon^{\mathrm{IV}}(\omega) = \sum_{j=1}^{3}\frac{f_j^2}{E_j^2-(\hbar\omega)^2-i\hbar\omega\Gamma_j}. \quad (9)$$

D. The frequency dependent damping

Damping constants in equations (1)-(9) are replaced with

$$\Gamma_i'(\omega) = \Gamma_i\exp\left[-\alpha_i\left(\frac{\hbar\omega-E_i}{\Gamma_i}\right)^2\right]. \quad (10)$$

In this way, shape of the line varies with ratio of parameters α_j and Γ_j. Lineshapes range from purely Lorentzian (for α=0) to nearly Gaussian ($\alpha = 0.3$), while for large α_j/Γ_j ratios wings of the peak in imaginary part of the dielectric function $\epsilon_2(\omega)$ are even narrower, thus enabling elimination of extended absorption tails in ϵ_2 which are characteristic for Lorentzian line shape. Since no broadening mechanism is set *a priori* (both α_j and Γ_j are adjustable model parameters) model becomes very flexible.

E. Complete model for the dielectric function

Dielectric function is obtained by summing up the contributions of all the above described critical points, with Γ replaced by $\Gamma'(\omega)$

$$\epsilon(\omega) = \epsilon_\infty + \epsilon^{\mathrm{I}}(\omega) + \epsilon^{\mathrm{II}}(\omega) + \epsilon^{\mathrm{III}}(\omega) + \epsilon^{\mathrm{IV}}(\omega), \quad (11)$$

where ϵ_∞ is the high-frequency dielectric constant containing the contributions of higher lying transitions.

III. Results and discussion

Position of the E_0 and $E_0+\Delta_0$, E_1 and $E_1+\Delta_1$ and their variation with composition x is accurately determined in the study of Kim *et al.* [12] The energies of these critical points are given with

$$E_i(x) = E_i(0)+(E_i(1)-E_i(0))x+(c_0+c_1x)x(1-x), \quad (12)$$

where values of $E_i(0), E_i(1), c_0$ and c_1 are listed in Table I. Therefore, energies of these CPs do not represent

TABLE II

MODEL PARAMETER VALUES

parameter	a_{0i}	a_{1i}	a_{2i}	a_{3i}
ϵ_∞	1.347	0.02	-0.568	4.210
A eV$^{1.5}$	3.06	14.210	-0.398	4.763
Γ_0 eV	0.0001	0.0107	-0.0187	0.3057
α_0	3.960	1.617	3.974	-5.413
B_1 eV	6.099	4.381	-4.718	-2.510
B_{1s} eV	0.001	0.103	4.447	0.208
B_{1x} eV	1.185	0.639	0.436	0.426
B_{2x} eV	0.473	0.770	-1.971	3.384
Γ_1 eV	0.194	0.125	-2.426	8.601
α_1	0.018	0.012	0.0035	0.310
f_2 eV	4.318	0.326	4.201	6.719
Γ_2 eV	0.496	0.597	-0.282	-0.139
α_2	0.014	0.281	-0.275	-0.569
E_2 eV	4.529	4.660	0.302	0.241
f_3 eV	4.924	5.483	-0.005	-0.337
Γ_3 eV	0.800	0.434	0.572	-0.553
α_3	0.032	0.052	-0.300	0.411
E_3 eV	4.746	4.710	-0.007	-0.565
f_4 eV	3.529	4.672	-6.226	0.643
Γ_4 eV	0.302	0.414	-0.414	1.136
α_4	0.004	0.023	-0.080	0.435
E_4 eV	4.860	4.976	-0.229	0.081

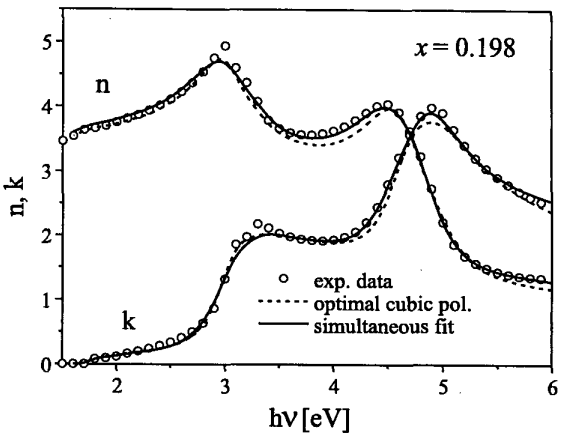

Fig. 1. The real and imaginary parts of the index of refraction for $x = 0.198$ as a function of energy; circles - experimental data, solid line - results obtained by simultaneous fit to all compositions, dashed line - results corresponding to model parameters calculated by optimal cubic polynomial obtained by fitting each composition separately.

adjustable parameters of the model. For other model parameters, each parameter is assumed to be cubic polinomial of composition x, in the form $a_{0i}(1-x) + a_{1i}x + (a_{2i} + a_{3i}x)x(1-x)$. No attempt was made to constrain the values during fitting procedure, except to avoid negative parameter values. The following objective function was employed

$$E(\mathrm{p}) = \sum_{j=1}^{j=N_x} \sum_{i=1}^{i=N_p} \left[\left| \frac{\epsilon_1(\omega_i, x_j) - \epsilon_1^{\mathrm{expt}}(\omega_i, x_j)}{\epsilon_1^{\mathrm{expt}}(\omega_i, x_j)} \right| + \left| \frac{\epsilon_2(\omega_i, x_j) - \epsilon_2^{\mathrm{expt}}(\omega_i, x_j)}{\epsilon_2^{\mathrm{expt}}(\omega_i, x_j)} \right| \right]^2 . \quad (13)$$

where N_p is number of experimental points, N_x is number of different compositions and $\epsilon_1(\omega_i, x_j)$, $\epsilon_2(\omega_i, x_j)$ are calculated values of real and imaginary part of the dielectric constant at frequency ω_i for composition x_j, while $\epsilon_1^{\mathrm{expt}}(\omega_i, x_j)$, $\epsilon_2^{\mathrm{expt}}(\omega_i, x_j)$ are the corresponding experimental values. The objective function was minimized by acceptance probability controlled simulated annealing algorithm with adaptive move-generation procedure, which is described in detail in [2].

Let us now explain the fitting procedures used. First, experimental data for individual compositions were fitted separately (the j in the outer sum in Eq.(13) was kept constant). After the optimal cubic polinomial describing the dependence of each parameter on composition x was determinated, it was found that such method can significantly compromise accuracy of the estimated dielectric function. This was already pointed out by Terry [16], but most other authors preferred the approach of finding optimal cubic polinomial after estimating parameters for each composition separately, since it is less time consuming and less computer resources demanding.

The simultaneous fit for all available compositions was employed next. This procedure was obviously more demanding on the optimization algorithm and also more computationaly intensive. The number of data points was larger approximatelly by an order of magnitude, and at the same time the number of fitting parameters was increased four times. Newertheless, this effort can be justified from the number of points. Firstly, the model parameter estimation does not give single, unique solution of the problem. Similar quality of approximation of experimental data can be obtained with different sets of parameters.

Another problem is illustrated in Fig. 1. This figure depicts two different calculated curves. Solid line is a result of best simultaneous fit accross all material compositions. Broken line is showing an interesting drawback of individual fitting. It is obtained by using cubic polinomial (cubic polinomial fit to parameters determined in individual fits). The descrepancies between the broken line and experimental data obviously reflect the difference between the cubic polynomial obtained in individual and simultaneous fits. It clearly shows the deterioration of the fit quality if optimal cubic polynomial is found after estimating parameters for each composition separately. Since main aim of modeling the optical properties of a ternary alloy is to enable calculation of the optical constants for compositions for which there are no available experimental data, it is clear that simulatenous approach to model parameter estimation for ternary alloy should be favoured. Therefore, in this work data sets for all available compositions were fitted simultaneously, giving best cubic coefficients to minimize discrepancies between calculated and experimental data over the entire energy and composition range.

The resulting coefficients are given in Table II. Excellent agreement with experimental data is obtained for the entire investigated spectral region and for all compositions.

Fig. 2 gives comparison between the model employed in this work (solid line) and conventional Adachi's model (broken line). Better agreement with experimental data ob-

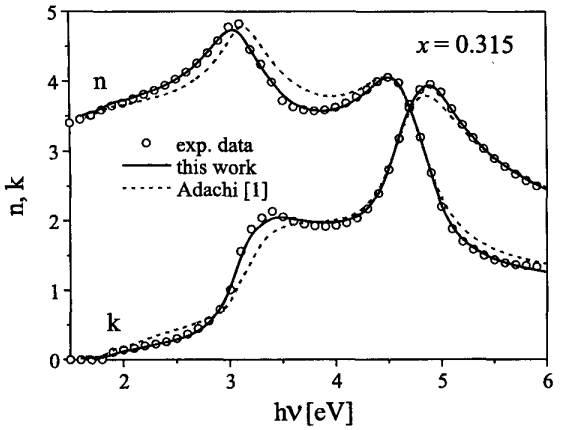

Fig. 2. Comparison with Adachi's model: the real and imaginary parts of the index of refraction *vs.* energy for $x = 0.315$; circles - experimental data, solid line - this work, broken line - Adachi, [Phys. Rev. B **38** , 12345 (1989)].

tained in this work, due to greater flexibility of the model achieved by frequency dependent damping mechanism and inclusion of the excitonic effects, can be clearly observed. In results presented here we didn't include contributions of the indirect tansitions since they exist only for $x > 0.45$ and their strength, since they represent second-order perturbation, should be significantly less. Fig. 3 shows the real and imaginary parts of the index of refraction *vs.* energy for compositions 0.3, 0.7 and 1.0. Obtained relative rms errors for the refractive index for our model with a total of 88 parameters are the largest for $x = 0.099$ and $x = 0.804$ (equal to 2.2%) and the lowest for $x = 0.315$ and $x = 0.419$ (equal to 1.4%). This is comparable to results of Kim *et al.*[12], who obtained rms errors below 2.5% with their model with 119 parameters, and results of Terry *et al.* who obtained rms errors below 3% with oscillator-based model with 144 parameters.

IV. Conclusion

Optical properties of $Al_xGa_{1-x}As$ are modeled in the 1.5-6 eV range for all compositions $0 \leq x \leq 1$. Extension of Adachi's model employing adjustable broadening function instead of the conventional Lorentzian one is used. This article discusses the significance of employing the experimental data for all compositions simultaneously for model parameter estimation. It is shown that this approach yields to more accurate and reliable results than those obtained by employing cubic polynomial for approximation of the composition dependence of parameters obtained by fitting each composition separately. Excellent agreement with experimental data, illustrated by relative rms error for refractive index below 2.2%, is obtained in the entire investigated spectral range and for all compositions. Total of 88 adjustable model parameters is employed, which is significantly lower compared to other studies giving similar quality of approximation of optical constants of $Al_xGa_{1-x}As$ in the 1.5-6 eV range.

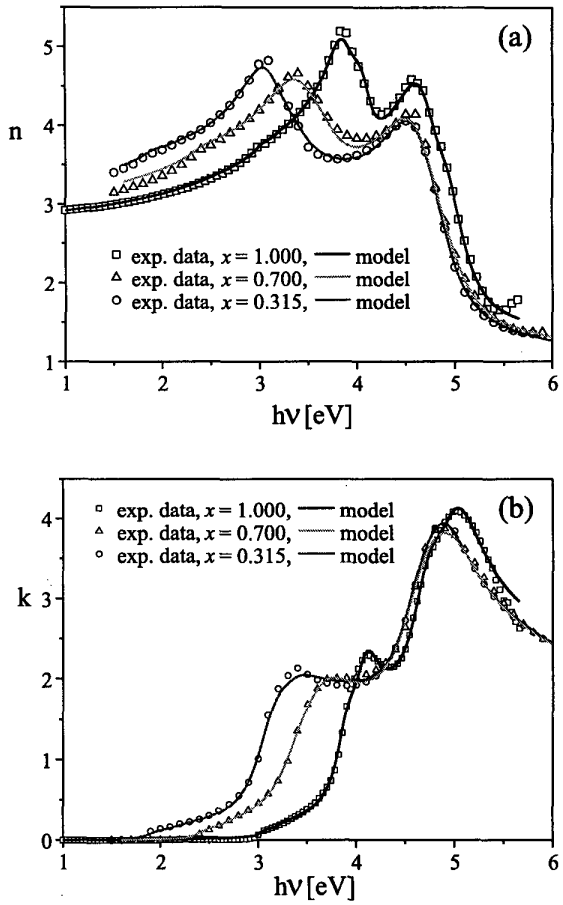

Fig. 3. The real (a) and imaginary (b) part of the index of refraction as a function of energy for compositions $x = 0.3$, 0.7 and 1.0.

References

[1] A. D. Rakić and M. L. Majewski, *J. Appl. Phys* **80**, 5509 (1996).
[2] A. D. Rakić, J. M. Elazar, and A. B. Djurišić. *Phys. Rev. E*, **52**, 6862 (1995).
[3] A. B. Djurišić,A. D. Rakić and J. M. Elazar, *Phys. Rev. E* **55**, 4797 (1997).
[4] S. Adachi, *J. Appl. Phys.* **53**, 5863 (1982).
[5] S. Adachi, *J. Appl. Phys.* **58**, R1 (1985).
[6] D. W. Jenkins, *J. Appl. Phys.* **68**, 1848 (1990).
[7] S. Adachi, T. Kimura and N. Suzuki, *J. Appl. Phys.* **74**, 3435 (1993).
[8] R. J. Deri and M. A. Emanuel, *J. Appl. Phys.* **74**, 3435 (1993).
[9] Y. Kokubo and I. Ohto, *J. Appl. Phys.* **81**, 2042, (1997).
[10] J. Zheng, C.-H. Lin and C. H. Kuo, *J. Appl. Phys.* **82**, 792 (1997).
[11] C. C. Kim, J. W. Garland, H. Abad and P. M. Raccah, *Phys. Rev. B* **45**, 11749 (1992).
[12] C. C. Kim, J. W. Garland, H. Abad and P. M. Raccah, *Phys. Rev. B* **47**, 1876 (1993).
[13] C. C. Kim and S. Sivananthan, *J. Appl. Phys.* **78**, 4003 (1995).
[14] O. Stenzel, R. Petrich, W. Scharff, A. Tikhonravov and V. Hopfe, *Thin Solid Films* **207**, 324 (1992).
[15] A. Franke, A. Stendal, O. Stenzel and C. von Borczyskowski, *Pure Appl. Opt.*, **5**, 845, (1996).
[16] F. L. Terry, Jr.,*J. Appl. Phys.*, **70**, 409 (1991).